

ОБЪЕДИНЕННЫЙ
ИНСТИТУТ
ЯДЕРНЫХ
ИССЛЕДОВАНИЙ
ДУБНА

E4-85-311

R.A.Eramzhyan,¹ T.D.Kaipov,² S.S.Kamalov

SPIN-DIPOLE EXCITATIONS
OF ${}^6\text{Li}$ IN CHARGED PION
PHOTOPRODUCTION

Submitted to "Zeitschrift für Physik"

¹ Institute of Nuclear Research,
USSR Academy of Sciences, Moscow, USSR

² Kazakh State University, 480091, Alma-Ata,
USSR

1985

1. INTRODUCTION

Excitation of the giant resonance is a universal response of atomic nuclei when various kinds of particles interact with them. The giant resonance is excited in photonuclear reactions, electron scattering, muon capture, radiative pion capture, inelastic hadron scattering, hadron charge exchange, etc. (see, for example, Ref.^{/1/}). The nuclear excitation in photoabsorption is of pure dipole type and it does not depend on spin of nucleons. In meson and hadron-nuclear reactions both spin-dependent and spin-independent transitions are of great importance. Under certain kinematical conditions the spin-isospin excitations dominate in the above-mentioned reactions. So, using the great variety of particles, one can get information on different modes of a giant resonance.

It is known that in very light nuclei the transitions of high multipolarity are fragmented strongly. Some concentration of the strength occurs mainly for dipole transitions. The gross-structure of a dipole resonance varies significantly going from one to another $1p$ -shell (${}^6\text{Li}$ - ${}^{16}\text{O}$) nucleus. Therefore, one must discuss each of them individually. Some features of dipole and spin-dipole resonances in $1p$ -shell nuclei have been discussed in Ref.^{/2-6/}. Experimental information on spin-dipole excitation has been extracted mainly from the data on radiative pion capture from mesoatomic orbits. But this reaction gives the data only at one fixed value of momentum transfer similar to photoabsorption reaction. The experimental data on pion photoproduction with excitation of spin-dipole resonance in some nuclei^{/7-10/} have become available recently. This opened the new possibilities in studying spin-dipole excitation. From the point of view of variation of momentum transfer, the (γ, π) reaction is analogous to inelastic electron scattering. However, for $1p$ -shell nuclei the inelastic electron scattering data concerning spin-dipole resonance region are known insufficiently. For that reason the (γ, π) -reaction is of great interest.

In the present paper we shall discuss the excitation of the spin-dipole resonance in ${}^6\text{Li}$ using the (γ, π) -reaction. By studying the inverse (π, γ) -process from mesoatomic orbits^{/4,5,11/}, some useful features of ${}^6\text{Li}$ excitation have been found out. The so-called configurational splitting and splitting due to the supermultiplet structure of the levels forming the dipole resonance are most interesting. The phenomenon is:

LIBRARY
UNIVERSITY OF TORONTO

i) the nucleonic transitions from the inner $1s$ - and outer $1p$ -shells are localized at different excitation energies and
 ii) transitions from the inner shell are also localized at different energies due to the difference in the Young scheme of the levels forming the giant resonance. The Young scheme (orbital) $[\lambda]$ is a model quantum number characterising the wave function symmetry under permutation of nucleons. In ${}^6\text{Li}$ the Young scheme is almost a good quantum number due to a significant contribution to a residual nucleon-nucleon interaction of the monopole part of Majorana force (see Ref.^{/2/}). The energy difference is large enough and a residual nucleon-nucleon interaction in nucleus is unable to remove it to form a single maximum. Such an effect has been predicted for the first time for the photonuclear reaction^{/13/}, and afterwards was extended for other reactions: muon and radiative pion capture^{/1,5,6/}.

We shall describe qualitatively the experimental data recently obtained for (n,p) -reaction^{/14/}. In this reaction both pure dipole and spin dipole resonances seem to be excited.

The nuclear levels which form the dipole and spin-dipole resonance in ${}^6\text{Li}$ are described in the framework of the bound shell model. The basis of the wave function for $J^\pi = 0^-, 1^-$ and 2^- ($T = 1$) levels includes all the configurations corresponding to nucleonic transitions within $1h\omega$ -excitation band. For levels $J^\pi T = 3^-1$ and 4^-1 we do not mix the configurations.

As follows from the previous studies the model used enables us to describe the gross-structure of excitation spectra^{/2,11/} only.

2. THE METHOD OF CALCULATIONS AND BASIC FORMULAE

2.1. Pion Photoproduction

The DWIA method is used as a rule for calculation of pion photoproduction on nuclei. When realizing this method we shall use the Lippmann-Schwinger form of the pion-nucleus wave function. The details of such an approach are given in Ref.^{/15/}. Here we summarize only a few working formulae.

The photoproduction amplitude on nuclei in total angular momentum J representation reads

$$F_{n0}^J(\pi, \gamma) = V_{n0}^J(\pi, \gamma) - \frac{1}{\pi} \sum_{n'\pi'} \int \frac{q'^2 dq'}{\mathfrak{M}_{n'}(q')} \frac{F_{nn'}^J(\pi, \pi') V_{n'0}^J(\pi', \gamma)}{\mathcal{E}_n(q) - \mathcal{E}_{n'}(q') + i\epsilon}. \quad (1)$$

The amplitude describes the photon absorption with quantum number $\gamma = (J_\gamma, k\lambda)$, where k is photon momentum, J_γ is its total angular momentum and λ is its polarization, and the pion creation with quantum number $\pi = (L_\pi, q)$, where L_π is pion angular mo-

mentum. The nucleus undergoes the transition from the ground $|0\rangle$ to excited $|n\rangle$ state.

The first term in (1)

$$V_{n0}^J(\pi, \gamma) = \langle L_\pi, q; J_n | V^J | J_\gamma, k\lambda; J_0 \rangle \quad (2)$$

is a plane wave part of the partial amplitude. The pion-nucleus interaction is taken into account in (1) by means of the second term. In (1) $\mathcal{E}_n(q) = E_\pi(q) + E_A^n(q)$ is the total energy of the pion and nucleus and $\mathfrak{M}_n(q)$ is the reduced mass. The pion-nucleus partial amplitude has been found from the solution of Lippmann-Schwinger equation. The details of these calculations are given in Refs.^{/15,16/}. When in (1) we put

$$n = n', \quad L_\pi = L'_\pi, \quad F_{nn}^J(\pi, \pi) = F_{00}^J(\pi, \pi), \quad (3)$$

we are thus led to the DWIA.

Next we shall use the approximation limiting the propagation of the pion on the energy shell. It means that instead of the full Green function

$$[\mathcal{E}_n(q) - \mathcal{E}_{n'}(q') + i\epsilon]^{-1} = \frac{\mathcal{P}}{\mathcal{E}_n(q) - \mathcal{E}_{n'}(q')} - i\pi\delta(\mathcal{E}_n(q) - \mathcal{E}_{n'}(q')) \quad (4)$$

we shall take its second term (on-shell approximation) only. It is well known^{/15/} that in on-shell DWIA, one frequently obtains numerical results which are rather close to both the calculations with the full Green function (4) and the experimental data.

The final expression for the pion photoproduction amplitude $F_{n0}^J(\pi, \gamma)$ in on-shell DWIA reads

$$F_{n0}^J(\pi, \gamma) = V_{n0}^J(\pi, \gamma) [1 + iq F_{00}^J(\pi, \pi)], \quad (5)$$

where $F_{00}^J(\pi, \pi)$ is the partial amplitude for pion-nucleus elastic scattering.

For the nucleonic photoproduction amplitude $f_{\pi\gamma}^\lambda$ needed to calculate $V_{n0}^J(\pi, \gamma)$ we use the CGLN^{/17/} one written in the form:

$$f_{\pi\gamma}^\lambda = if_1 \vec{\sigma} \cdot \vec{\epsilon} + f_2 [\hat{q} \times \hat{k}] \cdot \vec{\epsilon}_\lambda + if_3 \vec{\sigma} \cdot \hat{k} \hat{q} \cdot \vec{\epsilon}_\lambda + if_4 \vec{\sigma} \cdot \hat{q} \hat{q} \cdot \vec{\epsilon}_\lambda. \quad (6)$$

2.2. The Wave Functions of the Nuclear System with $A = 6$

The positive and negative parity states of $A = 6$ nuclear system have been described in the bound shell model. The positive parity wave functions for the levels with the configuration $1s^4 1p^2$ have been taken from Ref.^{/21/} In the ${}^6\text{Li}$ ground

state wave function the component $|1s^4 1p^2: ^{13}S_{1+}\rangle$ dominates. Therefore, in calculating all the transitions we have limited ourselves only to this component.

The wave functions of negative parity states with $J^\pi = 0^-, 1^-$ and 2^- and $T = 1$ have been taken from Ref. /11/. The corresponding wave functions have been obtained by diagonalising the residual nucleon-nucleon interaction using the complete $1h\omega$ -basis corresponding to $1s \rightarrow 1p$, $1p \rightarrow 2s$ and $1p \rightarrow 1d$ nucleonic transitions. The residual interaction has been chosen in the Rosenfeld form with the Gaussian radial dependence of the potential. The depth of the potential was equal to $V_0 = -60$ MeV. The positions of single-particle and single-hole states have been derived from experimental data on the neighbouring nuclei:

$$\epsilon(2s) - \epsilon(1p) = \epsilon(1d) - \epsilon(1p) = 12 \text{ MeV}, \quad \epsilon(1p) - \epsilon(1s^{-1}) = 24 \text{ MeV}. \quad (7)$$

To fix the position of negative parity states relative to the ground state of ^6Li the experimental parity data on the $^7\text{Li}(p, 2p)$ reaction have been used. Quasielastic process on $1s$ -nucleons in ^7Li results in the population of ^6He level at $E^* = 13.5$ MeV /22/ having the dominant configuration $|1s^{-1} 1p^3 [3]^{22} P: ^{33}P_{2-}\rangle$. Fixing the level position in such a way one can simultaneously explain some features of photonuclear reaction and muon capture on ^6Li /11/ especially of the $\gamma^6\text{Li} \rightarrow ^3\text{He}^3\text{H}$ and $\mu^6\text{Li} \rightarrow ^3\text{H}^3\text{He}$ disintegration channels. Spurious states due to the c.m. motion were eliminated by means of the Elliott-Skyrme technique. The wave functions are given in the Appendix. There are 15 levels with $J^\pi T = 2^- 1$, 14 with $J^\pi T = 1^- 1$, and 6 with $J^\pi T = 0^- 1$. We give the wave functions of those levels which carry a non-negligible strength in inelastic electron scattering.

We have not carried on the configuration mixing for the levels with $J^\pi T = 4^- 1$ and $3^- 1$. In $1h\omega$ -space there are three basic configurations $|1s^4 1p1d: ^{33}F_{-}\rangle$, $|1s^{-1} 1p^3 [21]^{24} D: ^{35}D_{4-}\rangle$ and $|1s^{-1} 1p^3 [3]^{22} F: ^{33}F_{4-}\rangle$ which form the wave functions of the $J^\pi T = 4^- 1$ levels. The energy difference between the first and the other two configurations is large enough not to mix them significantly. Moreover, the configurations with three nucleons in $1s$ -shell do not contribute to spin-dipole transitions due to the selection rules. So, only one $J^\pi T = 4^- 1$ level can be excited in the (γ, π) -reaction. We have assigned to it the wave function $|1s^4 1p1d: ^{33}F_{4-}\rangle$ and the energy E^* about 9 MeV.

On the contrast several basic configurations contribute to the wave functions of the $J^\pi T = 3^- 1$ levels. As follows from the selection rules only three of them contribute to the (γ, π) -reaction: $\psi_1 = |1s^4 1p1d: ^{33}F_{3-}\rangle$, $\psi_2 = |1s^4 1p1d: ^{31}F_{3-}\rangle$ and $\psi_3 = |1s^{-1} 1p^3 [21]^{24} P: ^{35}P_{3-}\rangle$.

The strongest transition is associated with the configuration ψ_3 thanks to the operator $j_1(Qr)[\sigma \otimes Y_1]_2$. The transitions associated with the first two configurations are due to the operators of the higher rank and therefore are weaker. The configurations with four nucleons in $1s$ -shell are separated in energy from configuration with three nucleons in $1s$ -shell significantly and again they mix weakly. Excitation energy of the level with configuration ψ_3 is about 24.5 MeV. The first two configurations are almost degenerated and therefore can be mixed strongly. However, we have not diagonalized them. Instead we considered them as describing two $J^\pi T = 3^- 1$ levels. We have assigned to them the excitation energy about 9 MeV.

3. THE RESULTS OF THE CALCULATION

3.1. The Photoproduction on ^6Li

The calculated ^6Li excitation spectra corresponding to pion photoproduction process at $k = 200$ MeV for four angles ($\theta = 30^\circ, 60^\circ, 90^\circ$ and 120°) are given in Fig. 1. In the calculated spectra one can separate several energy groups. The first is associated with $1p$ -nucleon transitions and is localized at excitation energies of ^6He from about 9 to 16 MeV. The contribution of levels with different $J^\pi T$ values to this excitation region depends on the momentum transfer, i.e., on the outgoing pion angle θ_π . At forward direction the $J^\pi = 2^- 1$ and $1^- 4$ levels are strongly excited. With increasing θ_π the contribution of the $J^\pi = 2^- 1$ level weakens rapidly, but the contribution of $J^\pi = 3^-$ and 4^- grows, see Table 1. For completeness, in Table 1 we give the results of calculations of transition strength to all low-lying levels of positive parity. The wave functions of Ref. /21/ were used for that purpose.

In the 9-16 MeV energy region one can see the nucleonic transitions from $1s$ -shell too. The wave functions of the corresponding levels have been constructed from the configurations carrying the highest symmetry (Young scheme) of $1p$ -shell nucleons, $1p^3 [3]$. Therefore, the excitation energy of such levels is not very high.

There is a group of transitions at about 20 MeV. It is created by the transitions of $1s$ -nucleons. However, the corresponding levels have lower symmetry for $1p$ -nucleons, namely $1p^3 [21]$, than the previous ones. Such transitions are localized in a wide energy interval.

Thus, the gross-structure of the giant resonances in pion photoproduction on ^6Li is due to splitting in the energy i) of nucleonic transitions from the inner and outer shells and ii) of nucleonic transitions from the outer $1p$ -shell resulting from the

Table 1

Differential cross section of pion photoproduction
on ${}^6\text{Li}$ (in $\mu\text{b/sr}$)

$J^\pi T$	$E^*({}^6\text{He}), \text{MeV}$	30°	60°	90°	120°	150°	
I	10,0	0,101	0,110	0,043	0,012	0,011	
2	13,0	0,427	0,604	0,500	0,309	0,192	
3	13,5	0,274	0,368	0,274	0,178	0,142	
1 ⁻ 4	15,5	0,812	1,08	0,890	0,584	0,404	
5	21,5	0,127	0,214	0,222	0,179	0,144	
6	22,5	0,246	0,334	0,306	0,225	0,169	
9	29,0	0,158	0,212	0,214	0,179	0,149	
I	11,0	0,888	0,984	0,488	0,142	0,039	
2	13,0	0,208	0,468	0,562	0,491	0,415	
2 ⁻ 6	20,5	0,398	0,577	0,590	0,489	0,399	
7	21,0	0,609	0,882	0,927	0,799	0,675	
10	29,5	0,412	0,515	0,495	0,406	0,332	
0 ⁻ 1	1	13,0	0,299	0,361	0,259	0,141	0,077
	3	23,0	0,124	0,162	0,150	0,113	0,086
3 ⁻ 1	1	9	0,005	0,040	0,127	0,173	0,163
	2	9	0,010	0,071	0,227	0,364	0,419
	3	21	0,746	1,096	1,139	0,965	0,807
4 ⁻ 1	1	9	0,007	0,066	0,213	0,318	0,335
0 ⁺ 1	1	0	2,04	0,372	0,002	0,047	0,070
	2	6,6	0,070	0,015	0	0,001	0,002
2 ⁺ 1	1	1,8	0,218	0,893	1,247	1,015	0,762
	2	4,2	0,041	0,061	0,072	0,059	0,045

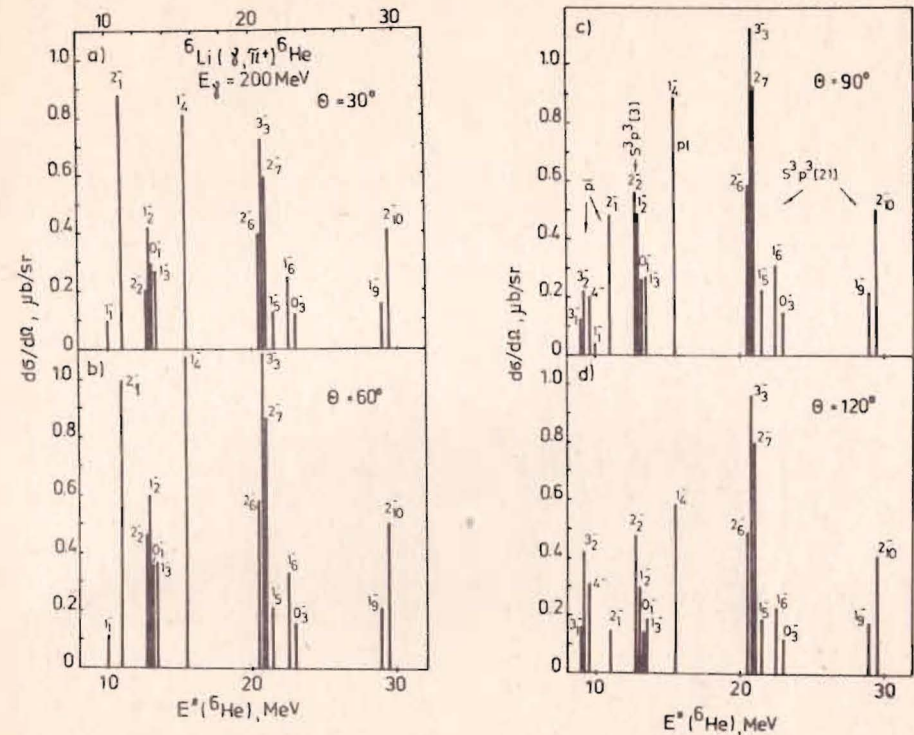


Fig.1. Calculated excitation spectra of ${}^6\text{Li}$ in (γ, π^+) -reaction at different angles of the outgoing pions.

splitting in the energy of levels with different Young schemes. The experimental data, Fig.2, indicate that there are several groups in the energy spectra too. However, their identification is far from being complete.

To elucidate more definitely the configurational splitting in ${}^6\text{Li}$, the coincidence measurements are needed. The outgoing pions in coincidence with α -particle separate the contribution of $1p$ nucleons to the reaction from that of $1s$ ones. In the last case α -particle cannot be emitted: either three-body decay takes place (for the states with Young scheme [21]) or two-body with two ${}^3\text{H}$ in the final state (for the states with Young scheme [3]). This decay channel is an analog of the decay channel to ${}^3\text{He} + {}^3\text{H}$ in photonuclear reaction and ${}^3\text{H} + {}^3\text{H}$ in muon capture^{/2/}.

As follows from the experimental data there are several groups of transitions in the ${}^6\text{Li}(\gamma, \pi^+){}^6\text{He}$ reaction. As the first group one can consider the transitions localized at $E^* = 7.9$ and 12 MeV. In the first and in the last cases the cross section

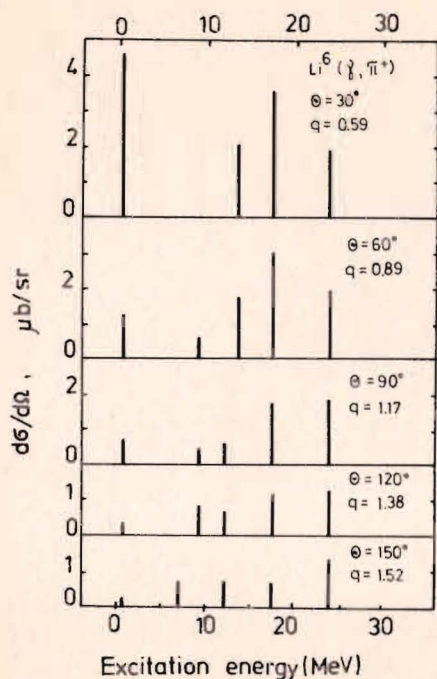


Fig. 2. Cross-structure of the experimental excitation spectra in the ${}^6\text{Li}(\gamma, \pi^+)$ reaction at different angles of outgoing pions ¹⁸⁾.

is large at backward pion angles; in the second case, at the forward. To this group there correspond the calculated transitions to the levels 3_1^- , 3_2^- , 4_1^- , 1_1^- and 2_1^- . All of them are located in the energy range from 9 to 11 MeV. The cross section of the $J^\pi = 3^-$ and 4^- levels increases when θ_π becomes larger. As to the levels $J^\pi = 1^-$ and 2^- the cross section decreases, see Fig. 3a. The theory seems to reflect qualitatively the experimental data. More detailed comparison between theory and experiment presents a problem both due to the limitation of

the model used and the large uncertainty of the experimental data. The same is true for all the groups of transitions.

The second group of transitions is located at $E^* = 13.6$ MeV. The angular distribution is peaked at forward angles. To this group one can assign the transitions to the levels $J^\pi = 2_2^-$, 1_2^- , 0_1^- and 1_3^- , see Fig. 3b. The third group of transitions is located at $E^* = 17.7$ MeV, Figure 3c. To this group one can assign the transitions to the levels $J^\pi = 1_4^-$, 2_6^- and 3_3^- . Let us emphasize that the separation of calculated transitions into the groups is somewhat arbitrary. We have no rigorous criterion to relate one or another level to the observed groups. The fourth group of transitions is localized at $E^* = 24$ MeV, see Fig. 3d. To this group one can assign the transitions to the levels $J^\pi = 2_7^-$, 1_5^- , 1_6^- and 0_3^- . After the grouping of the calculated transitions carried out in the above-mentioned way, the qualitative agreement with the measured angular distributions has been achieved. Nothing more can be extracted from the model used. The next step in description of pion photoproduction on ${}^6\text{Li}$ is connected with a direct consideration of the decay channels. The channel $\gamma + {}^6\text{Li} \rightarrow \pi + {}^3\text{H} + {}^3\text{H}$ considered in the same way as the channel $\gamma + {}^6\text{Li} \rightarrow {}^3\text{He} + {}^3\text{H}$ in Ref. ²²⁾. To calculate the three body-decay channels of ${}^6\text{Li}$, a more complicated approach is necessary. These can be the Faddeev equations with exclusion of the forbidden state in a way used in Ref. ²³⁾.

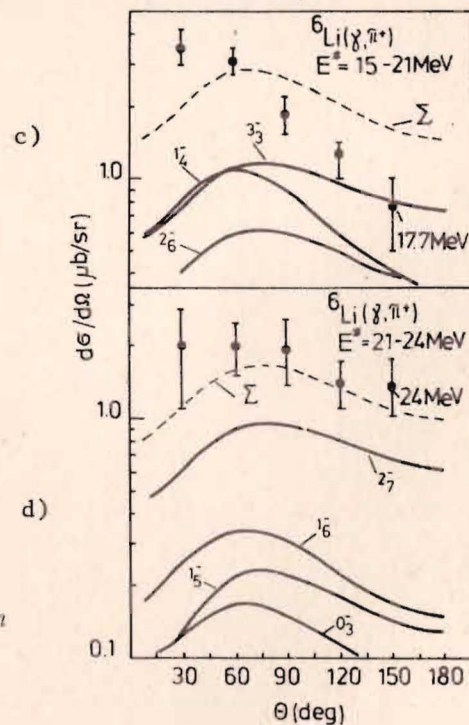
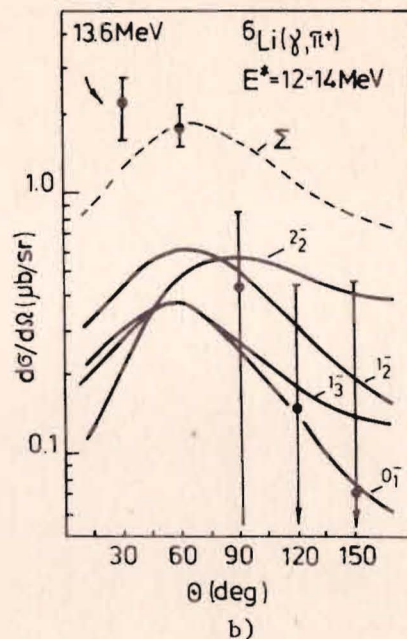
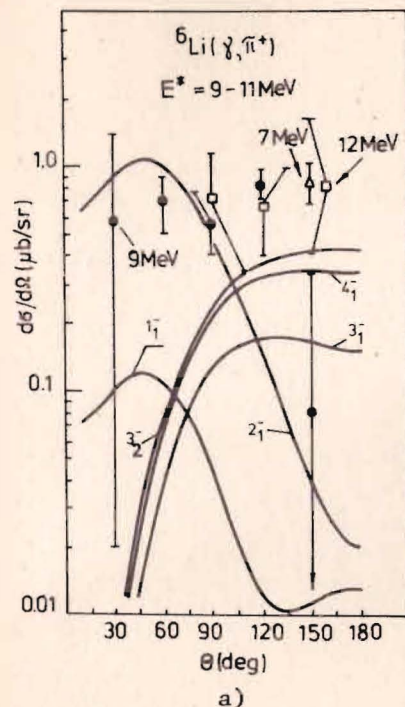


Fig. 3a-d. Angular distribution of the outgoing pions when different energy regions of ${}^6\text{He}$ are excited.

3.2. Comparison of ${}^6\text{Li}$ Excitation Spectra in the Pion Photoproduction Reaction and in Some Other Reactions

A) Inelastic electron scattering.

In ${}^6\text{Li}$ as in other 1p-shell nuclei^{/6/} theory predicts some concentration of M2- and E1-transitions. The M2-resonance, see Fig.4, is formed of a few strong transitions.

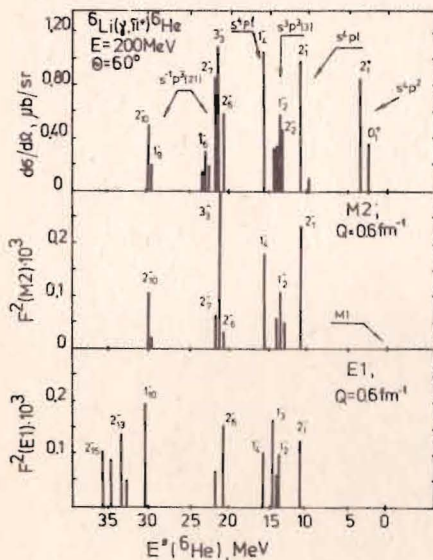


Fig.4. Spin-dipole transitions in ${}^6\text{Li}$ in inelastic electron scattering (E1 and M2-transitions) and in pion photoproduction reaction. For levels $J^\pi T = 2^-1$ $F^2(E1) \times 0.5 \times 10^{-3}$.

As in the (γ, π) -reaction the low-energy part of M2-resonance is associated predominantly with 1p-nucleonic transitions. The intensity of 1s-nucleonic transition forming the final states with the highest [3] symmetry ($1s^{-1} 1p^3[3]$) is lower than the intensity of 1p-nucleonic transitions. In the energy region above 20 MeV the nucleonic transitions from 1s-state dominate.

Strongly populated is the $J^\pi = 3^-3$ level. The same level forms the main maximum in the (γ, π) -reaction.

Transversal electric dipole transitions (E1) are spread over large energy region and are shifted to high energies. The E1-transitions are due to both the convective and magnetization current. From the point of view of the (γ, π) -reaction the information on magnetization current is needed. Therefore in Table 2, where the form factors of E1 transitions are given, one can find the contributions of magnetization current.

The same nuclear states form the low-energy branch of both E1- and M2-resonance in ${}^6\text{Li}$. The same states are active in the (γ, π) -reaction. The high energy branch of E1-resonance is built of different states than the same branch of M2-resonance. Moreover, in E1-transitions the energy region above 30 MeV is strongly populated. However, the contribution of the magnetization current to this high energy region is not high as it can be seen from Table 2. Therefore, this region is weakly populated in the (γ, π) -reaction. That is why the gross-structure of excitation in the (γ, π) -reaction is very similar to the gross-structure of M2-excitation.

Table 2

Inelastic form factors of ${}^6\text{Li}$. - $F^2(E1; Q = 0.6 \text{ fm}^{-1}) \times 10^4$; a) without continuity equation; b) using the continuity equation /18,19/; c) the contribution of magnetization current to the form factor

No.	$J^\pi T = 2^-1$			$J^\pi T = 1^-1$			$J^\pi T = 0^-1$		
	a	b	c	a	b	c	a	b	c
	MeV								
I	14,5	3,04	I,11	16,5	1,07	1,02	16,5	1,34	I,30
2	16,5	0,39	0,08	17,0	1,80	1,69	18,5	0,22	0
3	19,0	0,27	0,02	19,0	0,98	0,95	26,5	0,28	0,54
6	24,0	2,36	2,98	25,0	0,50	0,51	32,5	0,28	0,33
7	24,5	1,45	1,15	26,0	0,42	0,16	33,5	0,01	0,10
10	33,0	0,38	0,23	28,0	0,06	0,17	0		
11	35,0	0,11	0,19	32,5	0,16	0,002	0,54		
12	36,5	0,19	0,90	33,5	0,46	2,01	0		
13	37,0	0,67	2,81	35,5	0,18	0,31	0,10		
14	39,0	0,40	1,64	41,5	0,11	0,12			
15	40,0	0,40	1,81						

B) Neutron charge-exchange reaction, photoabsorption, and radiative pion capture from the mesoatomic orbits

The experimental and calculated excitation spectra of ${}^6\text{Li}$ in radiative pion capture from the mesoatomic orbits are compared with the experimental spectra in the (n,p)-reaction at incident neutron energy $T_n = 59.6 \text{ MeV}^{14/}$ in Fig.5a. The calculated excitation spectra in photoabsorption on ${}^6\text{Li}$ and in the (γ, π)-reaction are given in Fig.5b.

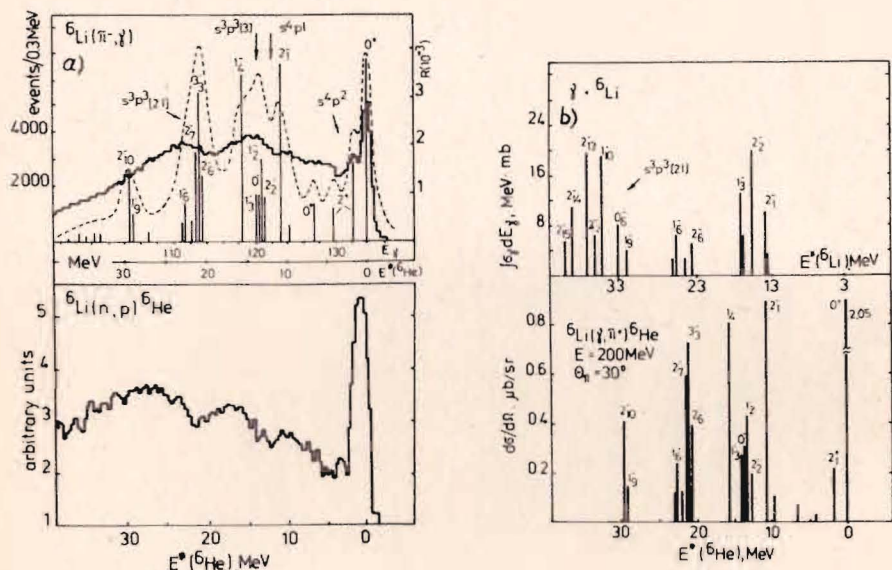


Fig.5. Excitation spectra of ${}^6\text{Li}$ in: a) the (π^-, γ) - and $(n, p)^{14/}$ reactions; b) in the (γ, π^+) reaction and photoabsorption.

As follows from Fig.5 the gross-structure of excitation spectra in reactions under the discussion is more or less similar. First of all it is so since it is formed of the dipole and spin dipole transitions. At the same time there is some difference in spectra. The high energy part of the excitation spectra is more intensively populated in the (n,p) reaction and in photoabsorption as compared to the (π, γ) reaction. In the (n,p) reaction at $T_n = 59.6 \text{ MeV}$ the contribution of pure dipole excitation is strong enough. Therefore, the high energy part of excitation spectra in this reaction should be very close to high energy part of photonuclear reaction.

The low energy part of photonuclear and spin-dipole resonance is formed by the same states. Therefore, the structure of the excitation spectra in all four reactions is similar in the low energy region.

4. CONCLUSION

We have studied the excitation of dipole and spin-dipole resonance in ${}^6\text{Li}$ by various kinds of particles: photons, electrons, pions and neutrons. Using the bound shell model for the description of nuclear states we have shown that the gross-structure of a resonance for each particle is governed by the configurational splitting: nucleonic transitions from outer and inner shells are located in different energy regions and overlap very weakly. At the same time there is an additional splitting in the transitions from the outer shell which is due to splitting of the final states according to the Young scheme.

The analysis performed allows one to explain uniquely the observed spectra of ${}^6\text{Li}$ excited by various kinds of particles. The results obtained have the semiquantitative nature for the reasons discussed in the text. For the quantitative description one needs to go beyond the bound shell model. Nevertheless, the results obtained in the model used allow one to elucidate the most important feature of the response of this nucleus when it interacts with different particles.

The authors wish to acknowledge Dr. O.Sasaki for providing with the experimental data before publication and Prof. K.Shoda for a fruitful discussion of the results of measurements.

APPENDIX

The wave functions of negative parity are built up of the configurations

$$|1s^4 1p1d: {}^{2T+1, 2S+1}L_2\rangle = |d: {}^{2T+1, 2S+1}L_2\rangle,$$

$$|1s^4 1p2s: {}^{2T+1, 2S+1}L_2\rangle = |s: {}^{2T+1, 2S+1}L_2\rangle,$$

where T, S and L are isospin, spin and angular momentum of A = 6 nuclear system and of the configuration

$$\begin{aligned} & |1s^{-1} 1p^3 [\lambda_2] \begin{matrix} 2T_2+1, 2S_2+1 \\ L_2 \end{matrix} \begin{matrix} 2T+1, 2S+1 \\ L_2 \end{matrix} \rangle \\ & = |[\lambda_2] \begin{matrix} 2T_2+1, 2S_2+1 \\ L_2 \end{matrix} \begin{matrix} 2T+1, 2S+1 \\ L_2 \end{matrix} \rangle, \end{aligned}$$

where T_2 , S_2 , $[\lambda_2]$ and L_2 are the isospin, spin, Young scheme and angular momentum of three nucleons in $1p$ -shell. The coupling of momenta is as follows: $\vec{S} + \vec{L} = \vec{J}$. We give the components with the amplitude $a > 0.20$. The energies of levels are given in Tables 1 and 2.

1. The wave functions of the $J^\pi T = 1^-1$ levels

$$\begin{aligned} \Psi(1_1^-) &= 0.594 |s: {}^{31}P\rangle - 0.443 |s: {}^{33}P\rangle - 0.421 |d: {}^{31}P\rangle + \\ &+ 0.299 |[21] {}^{42}P: {}^{31}P\rangle - 0.328 |d: {}^{33}P\rangle + 0.229 |[3] {}^{22}P: {}^{31}P\rangle \\ \Psi(1_2^-) &= 0.831 |[3] {}^{22}P: {}^{33}P\rangle - 0.332 |s: {}^{33}P\rangle - 0.259 |s: {}^{31}P\rangle - 0.243 |d: {}^{33}P\rangle \\ \Psi(1_3^-) &= 0.364 |s: {}^{31}P\rangle + 0.446 |[3] {}^{22}P: {}^{31}P\rangle - 0.501 |s: {}^{33}P\rangle + \\ &+ 0.386 |d: {}^{33}P\rangle + 0.497 |[3] {}^{22}P: {}^{33}P\rangle \\ \Psi(1_4^-) &= 0.615 |d: {}^{31}P\rangle + 0.605 |[3] {}^{22}P: {}^{31}P\rangle - 0.356 |s: {}^{33}P\rangle \\ \Psi(1_5^-) &= 0.980 |[21] {}^{24}P: {}^{35}P\rangle \\ \Psi(1_6^-) &= -0.277 |s: {}^{33}P\rangle + 0.577 |d: {}^{33}P\rangle - 0.212 |[21] {}^{22}P: {}^{33}P\rangle + \\ &+ 0.210 |[21] {}^{24}P: {}^{33}P\rangle + 0.606 |[21] {}^{42}P: {}^{33}P\rangle \\ \Psi(1_7^-) &= 0.235 |[21] {}^{22}P: {}^{33}P\rangle + 0.935 |[21] {}^{24}D: {}^{35}D\rangle \\ \Psi(1_8^-) &= -0.470 |[21] {}^{22}P: {}^{33}P\rangle + 0.579 |[21] {}^{24}P: {}^{33}P\rangle - 0.577 |[21] {}^{42}P: {}^{33}P\rangle \\ \Psi(1_{10}^-) &= -0.763 |[21] {}^{22}P: {}^{33}P\rangle - 0.566 |[21] {}^{24}P: {}^{33}P\rangle + 0.228 |[21] {}^{24}D: {}^{35}D\rangle \\ \Psi(1_{12}^-) &= 0.615 |[21] {}^{22}P: {}^{31}P\rangle - 0.292 |[21] {}^{42}P: {}^{31}P\rangle + 0.454 |[21] {}^{22}D: {}^{33}D\rangle + \\ &+ 0.529 |[21] {}^{24}D: {}^{33}D\rangle \\ \Psi(1_{13}^-) &= -0.614 |[21] {}^{22}P: {}^{31}P\rangle + 294 |[21] {}^{42}P: {}^{31}P\rangle + 0.614 |[21] {}^{24}D: {}^{33}D\rangle - \\ &- 0.265 |[21] {}^{42}D: {}^{33}D\rangle \end{aligned}$$

2. The wave functions of the $J^\pi T = 2^-1$ levels

$$\begin{aligned} \Psi(2_1^-) &= -0.665 |s: {}^{33}P\rangle - 0.584 |d: {}^{33}P\rangle + 0.332 |[3] {}^{22}P: {}^{33}P\rangle - 0.242 |d: {}^{31}D\rangle \\ \Psi(2_2^-) &= 0.912 |[3] {}^{22}P: {}^{33}P\rangle + 0.217 |d: {}^{31}D\rangle + 0.205 |s: {}^{33}P\rangle \\ \Psi(2_3^-) &= -0.684 |d: {}^{31}D\rangle + 0.320 |s: {}^{33}P\rangle + 0.300 |[21] {}^{42}D: {}^{31}D\rangle + 0.517 |d: {}^{33}F\rangle \\ \Psi(2_6^-) &= 0.613 |[21] {}^{42}P: {}^{33}P\rangle + 0.464 |d: {}^{33}P\rangle + 0.395 |[21] {}^{24}P: {}^{35}P\rangle - \\ &- 0.351 |d: {}^{33}P\rangle + 0.213 |[21] {}^{24}P: {}^{33}P\rangle \\ \Psi(2_7^-) &= 0.901 |[21] {}^{24}P: {}^{35}P\rangle - 0.286 |[21] {}^{42}P: {}^{33}P\rangle \\ \Psi(2_{10}^-) &= 0.878 |[21] {}^{22}P: {}^{33}P\rangle + 0.282 |[21] {}^{42}P: {}^{33}P\rangle - 0.230 |d: {}^{33}P\rangle \\ \Psi(2_{11}^-) &= -0.849 |[21] {}^{22}D: {}^{33}D\rangle - 0.408 |[21] {}^{42}D: {}^{33}D\rangle \\ \Psi(2_{12}^-) &= 0.277 |[21] {}^{22}P: {}^{33}P\rangle + 0.302 |[21] {}^{24}P: {}^{33}P\rangle + 0.310 |[21] {}^{22}D: {}^{33}D\rangle + \\ &+ 0.751 |[21] {}^{24}D: {}^{33}D\rangle - 0.338 |[21] {}^{42}D: {}^{33}D\rangle \\ \Psi(2_{13}^-) &= 0.531 |[21] {}^{24}P: {}^{33}P\rangle - 0.232 |[21] {}^{42}P: {}^{33}P\rangle - 0.281 |[21] {}^{22}D: {}^{31}D\rangle - \\ &- 0.229 |[21] {}^{22}D: {}^{33}D\rangle - 0.226 |[21] {}^{24}D: {}^{33}D\rangle + 0.639 |[111] {}^{44}S: {}^{35}S\rangle \\ \Psi(2_{14}^-) &= -0.410 |[21] {}^{24}P: {}^{33}P\rangle + 0.279 |[21] {}^{42}P: {}^{33}P\rangle + \\ &+ 0.381 |[21] {}^{22}D: {}^{31}D\rangle + 0.742 |[111] {}^{44}S: {}^{35}S\rangle \\ \Psi(2_{15}^-) &= -0.396 |[21] {}^{24}P: {}^{33}P\rangle + 0.236 |[21] {}^{42}P: {}^{33}P\rangle - \\ &- 0.758 |[21] {}^{22}D: {}^{31}D\rangle + 0.350 |[21] {}^{42}D: {}^{31}D\rangle \end{aligned}$$

REFERENCES

1. Balashov V.V., Korenman G.Ya., Eramzhyan R.A. Meson Capture by Atomic Nuclei. (in Russian). Atomizdat, M., 1978.
2. Ishkhanov B.S. et al. Sov.J.Part. and Nucl., 1981, 12, p.905.
3. Goncharova N.G., Kissener H.R., Eramzhyan R.A. Sov.J. Part. and Nuclei, 1985, 16.
4. Gmitro M. et al. Sov.J.Part. and Nucl., 1983, 14, p.773; Preprint of Physik Institut der Universität, Zurich.
5. Kissener H.R. et al. Nucl.Phys., 1978, A312, p.394.
6. Eramzhyan R.A., Gmitro M., Kissener H.R. Nucl.Phys., 1980, A338, p.436.
7. Shoda K. et al. Photopion Nuclear Physics. (Ed. by P.Stoler). Plenum Press, New York and London, 1978, p.205.
8. Sasaki O. et al. Contributed papers to International Symposium on Nuclear Spectroscopy and Nuclear Interactions. Osaka, 1984.
9. Min K. et al. Phys.Rev.Lett., 1980, 44, p.1384.
10. Min K. et al. Phys.Rev., 1983, C28, p.464.
11. Sakaev R.A., Eramzhyan R.A. JINR, P2-9610, Dubna, 1976.
12. Bohr A., Mottelson B.R. Nuclear Structure. (Ed. by W.A.Benjamin). New York, Amsterdam, 1974.
13. Neudachin V.G., Smirnov Yu.F. Nucl.Phys., 1965, 66, p.25.
14. Brady F. et al. Phys.Rev.Lett., 1983, 51, p.1320.
15. Eramzhyan R.A. et al. J.Phys., 1983, G9, p.605; Eramzhyan R.A. et al. Nucl.Phys., 1984, A429, p.403.
16. Gmitro M., Mach R. Z.Phys.A - Atoms and Nuclei, 1979, 290, p.179; Gmitro M., Kvasil J., Mach R. Phys.Lett., 1982, 113B, p.205.
17. Chew G.F. et al. Phys.Rev., 1957, 106, p.1345.
18. Eisenberg J.M., Greiner W. Nucl.Theory. North-Holland, Amsterdam, 1970, vol.2.
19. Gmitro M., Kaipov T.D., Rizek J. JINR, P4-84-443, Dubna, 1984.
20. Petrovich F., Love W.G. Nucl.Phys., 1981, A354, p.499.
21. Boyarkina A.N. Izv.Akad.Nauk SSSR, ser.fiz., 1964, 28, p.337.
22. Tyren H., Kullander S., Sundberg O. Nucl.Phys., 1966, 79, p.321.
23. Burkova N.A., Zhusupov M.A. Contributed papers to International Conference on Nuclear Physics. Florence, 1983, p.C27.
24. Kukulin V.I., Neudachin V.G., Smirnov Yu.F. Sov.J.Part. and Nuclei, 1979, 10, p.1236.

Received by Publishing Department
on April 29, 1985.

Эрамжин Р.А., Каипов Т.Д., Камалов С.С. E4-85-311
Спин-дипольные возбуждения ${}^6\text{Li}$
в реакции фоторождения заряженных пи-мезонов

В рамках модели оболочек рассчитаны сечения фоторождения заряженных пи-мезонов на ядре ${}^6\text{Li}$ с возбуждением спин-изоспинового дипольного резонанса. Показано, что gross-структура спектра возбуждения ядерной системы в ${}^6\text{Li}(\gamma, \pi)$ -реакции обусловлена конфигурационным расщеплением резонанса. Выявлены области концентрации переходов. Проведено сравнение спектра возбуждения ${}^6\text{Li}$ в (γ, π) -реакции и в реакциях (π, γ) , (e, e') и (n, p) , в которых также преобладают спин-изоспиновые переходы.

Работа выполнена в Лаборатории теоретической физики ОИЯИ.

Препринт Объединенного института ядерных исследований, Дубна 1985

Eramzhyan R.A., Kaipov T.D., Kamalov S.S. E4-85-311
Spin-Dipole Excitations of ${}^6\text{Li}$
in Charged Pion Photoproduction

In the framework of bound shell model we have calculated the photoproduction of charged pions on ${}^6\text{Li}$ when spin-isospin dipole resonance is excited. It is shown that the transition strength concentrates in several energy regions. Such a gross-structure of the excitation spectrum is governed by the configurational splitting of the resonance. The excitation spectrum in ${}^6\text{Li}(\gamma, \pi)$ -reaction is compared with the ${}^6\text{Li}(\pi, \gamma)$, (e, e') and (n, p) reaction spectra where spin-isospin transitions are dominating too.

The investigation has been performed at the Laboratory of Theoretical Physics, JINR.

Preprint of the Joint Institute for Nuclear Research. Dubna 1985